The Astronomical Journal, 134:2353–2365, 2007 December

CONTACT BINARIES WITH ADDITIONAL COMPONENTS. III.[1] A SEARCH USING ADAPTIVE OPTICS

Slavek M. Rucinski,[2] Theodor Pribulla,[3] and Marten H. van Kerkwijk[2]

Received 2007 June 4; accepted 2007 August 14

ABSTRACT

We present results of the Canada-France-Hawaii Telescope adaptive optics (AO) search for companions of a homogeneous group of contact binary stars, as a contribution to our attempts to prove the hypothesis that these binaries require a third star to become as close as observed. In addition to directly discovering companions at separations of $\geq 1''$, we introduced a new method of AO image analysis utilizing distortions of the AO diffraction ring pattern at separations of $0.07''$–$1''$. Very close companions, with separations in the latter range, were discovered in the systems HV Aqr, OO Aql, CK Boo, XY Leo, BE Scl, and RZ Tau. More distant companions were detected in V402 Aur, AO Cam, and V2082 Cyg. Our results provide a contribution to the mounting evidence that the presence of close companions is a very common phenomenon for very close binaries with orbital periods <1 day.

Key words: binaries: close — binaries: eclipsing — stars: variables: other

Online material: extended figure sets, machine-readable table

1. INTRODUCTION

The formation of close binaries is still a puzzle: How can they be formed if the components were larger than the instantaneous orbit during the pre-main-sequence phase? One possibility is that angular momentum transfer to a third companion caused the originally wider orbit to shrink during the main-sequence (MS) phase. If this hypothesis is true, all close binaries should be accompanied by a third body (unless it was removed by an encounter, but this is unlikely by the time the stars have reached the MS). Thus, one would expect the incidence of the triples to be higher than in a sample of relatively wide ($P \gtrsim 10$ days) binaries. Tokovinin & Smekhov (2002) and Tokovinin et al. (2006) studied the frequency of occurrence of tertiary companions for the binary period range of 1–30 days and collected an impressive amount of evidence that indeed the frequency of tertiaries increases as the binary period decreases, from a level of about 34% for orbital periods of 12–30 days to 50% at 9 days, and further to perhaps even 100% at 1 day.

This paper is the third in a series assessing the presence and properties of tertiary companions to very close binaries with periods shorter than 1 day. In the first paper of the series, Pribulla & Rucinski (2006, hereafter Paper I), we summarized the present state, collecting all detections of third and/or multiple components of contact binaries. This led to a heterogeneous sample, with observational biases which were difficult to quantify. Nevertheless, for our sample of contact binaries brighter than $V_{\max} = 10$, it allowed us to set a firm lower limit of $59\% \pm 8\%$ to the incidence of tertiaries (for the better observed subsample of the northern hemisphere systems). The preliminary results of the adaptive optics (AO) program discussed in the current paper were reported in Paper I.

In D'Angelo et al. (2006, hereafter Paper II) we presented a spectroscopic search for faint third components. Several thousand medium-resolution spectra obtained during the David Dunlap Observatory (DDO) radial velocity program for 80 binaries were reanalyzed, and weak, but stable, spectral signatures of tertiaries were searched for in the averaged spectra. This resulted in a detection of 15 tertiaries—of which 11 were previously unknown—in a homogeneous sample of 59 contact binaries. The continuation of the radial velocity observations—110 good accuracy orbits are now published (Pribulla et al. 2007)—will provide material for a future similar study. The spectroscopic observations permit detection of very close companions hidden in the seeing disk of close binaries (at DDO typically $1.8''$–$2''$) but, for faint companions, detection is limited to a magnitude difference of about 5 mag [e.g., in CK Boo, $L_3/(L_1 + L_2) = 0.009$; Paper II]. The AO observations presented in the current paper permit detection of much fainter and redder companions, particularly in the infrared, but only at relatively large separations, and with long-period orbits, compared to those studied spectroscopically. Unlike for spectroscopic observations, where a physical bond can often be proven by similar systemic velocities or mutual revolution, visual detections for nearby (<300 pc) and relatively bright ($V < 10$) binaries may suffer some contamination from projections; often, however, the density of background stars is sufficiently low that the mere presence of an object at small separation from a bright star is a strong indication of a physical bond.

The majority of the systems covered in this series of papers are genuine contact binaries. At orbital periods shorter than 1 day they are the most frequently detected and studied. However, our program also includes binaries with unequally deep eclipses which may be contact binaries with poor thermal contact or short-period semidetached systems. In some cases (V1464 Aql and TT Cet), low photometric amplitudes and/or the lack of spectroscopic observations preclude any meaningful classification. We note that, in terms of evolution, all these types must be related to contact binaries as binaries of the least orbital angular momentum. Hence, we will interchangeably use the terms "close" and "contact" binary stars throughout this paper to mean all target binaries with periods shorter than 1 day.

This paper is structured in the following way: In § 2 we describe our observations and their reduction, and in § 3 we introduce a new search technique for multiples, which uses template fitting, and present our new detections. In § 4 we use a Monte Carlo technique to verify our estimate of the detection limits for a given magnitude difference. In § 6 we present tests of the physical bond

[1] Based on observations obtained at the Canada-France-Hawaii Telescope, which is operated by the National Research Council of Canada, the Institut National des Sciences de l'Univers of the Centre National de la Recherche Scientifique of France, and the University of Hawaii.

[2] Department of Astronomy, University of Toronto, 50 St. George Street, Toronto, ON M5S 3H4, Canada; rucinski@astro.utoronto.ca, mhvk@astro.utoronto.ca.

[3] Astronomical Institute, Slovak Academy of Sciences, 059 60 Tatranská Lomnica, Slovakia; pribulla@ta3.sk.

TABLE 1

AO Observations during the Three Observing Runs of 1998 January 10 and July 23, and 2005 October 17–18

Frame No.	Object	HJD − 2,400,000	Filter
419979	AQ Psc	50,824.7062	K_{CO}
419980	AQ Psc	50,824.7081	K_{CO}
419981	AQ Psc	50,824.7100	K_{CO}
419982	AQ Psc	50,824.7122	K_{CO}
419983	AQ Psc	50,824.7144	K_{CO}
419984	AQ Psc	50,824.7165	K_{CO}
419985	AQ Psc	50,824.7184	K_{CO}
419986	AQ Psc	50,824.7203	K_{CO}
419987	TT Cet	50,824.7291	K
419988	TT Cet	50,824.7316	K

Notes.—Table 1 is published in its entirety in the electronic edition of the *Astronomical Journal*. The first 10 rows are shown here for guidance regarding its form and content. The central wavelengths and bandwidths of the filters used are as follows: (K_{CO}) $\lambda_{cen} = 2.298$ μm, FWHM $= 0.027$ μm; (K) $\lambda_{cen} = 2.22$ μm, FWHM $= 0.4$ μm; (H) $\lambda_{cen} = 1.65$ μm, FWHM $= 0.29$ μm; (H_2) $\lambda_{cen} = 2.122$ μm, FWHM $= 0.02$ μm. The K_{CO} filter is entered as "CO" in the machine-readable version of the table.

between the visual companions, and in § 7 we discuss the nature of the detected companions. Finally, in § 8 we summarize and interpret our results.

2. OBSERVATIONS

We obtained observations aimed at the direct detection of companions of contact binary stars on the nights of 1998 January 10 and July 23, and 2005 October 17 and 18 using the AO system at the Canada-France-Hawaii Telescope (CFHT). During the 2005 run, the specific goal was to survey the many bright contact binaries originally detected by the *Hipparcos* satellite and later confirmed spectroscopically during radial velocity programs (mostly at the DDO; for reference, see Pribulla et al. 2006, 2007). Altogether, 80 known contact binary stars—accessible from CFHT to an approximate limit of $V < 10.5$—were observed, with 15 objects observed on two occasions and two objects observed three times. The journal of all observations can be found in Table 1, and an overview of the detections is given in Table 2.

We used the PUEO AO system with the KIR camera combination (Rigaut et al. 1998), with a 1024×1024 pixel detector that covers a field of $36'' \times 36''$ at a scale of $0.0348''$ pixel^{-1}. In 1998 most of the observations were done in the infrared K band or, to avoid overexposure of the contact binary, a narrowband filter centered on the CO bands (K_{CO}; for details on the filters, see the notes to Table 1); a few binaries were also observed in the H band (1.65 μm). In 2005 we used the H_2 filter, which for our purposes is effectively another narrowband K filter.

In 1998 each source was observed by positioning it in each of the four quadrants of the detector, while in 2005 a fifth, central position was added. At each position, typically three to five exposures with integration times from 5 to 40 s were obtained; typically, we thus collected 12–25 individual images. With the image shifts and multiple exposures, we could obtain good definitions of the background and, for detected visual companions, reliable uncertainty estimates of magnitude differences (Δm), separations (ρ), and position angles (P.A., θ).

In all cases, the contact binaries themselves were sufficiently bright to be used for sensing the distortion of the wave front and deriving the AO corrections. In the K passband, the isoplanatic

TABLE 2

Overview of Observed Systems and Detections of Visual Companions

Object	Detection	Object	Detection	Object	Detection
AB And	-NN	RW Com	N--	V753 Mon	--N
GZ And	-DD	RZ Com	N--	V502 Oph	-N-
V376 And	--N	SX Crv	-N-	V508 Oph	-D-
EL Aqr	-N-	CV Cyg	--N	V566 Oph	-NN
HV Aqr	--D	DK Cyg	-NN	V839 Oph	-N-
OO Aql	--D	V401 Cyg	-NN	V2388 Oph	--C
V417 Aql	-N-	V1073 Cyg	-NN	ER Ori	D-N
V1464 Aql	--N	V2082 Cyg	--D	V1363 Ori	--N
AH Aur	D-D	LS Del	--N	U Peg	-DD
V402 Aur	--D	SV Equ	-N-	BB Peg	-NN
V410 Aur	--D	UX Eri	N--	V335 Peg	--N
V449 Aur	--N	YY Eri	N-N	V351 Peg	--N
TZ Boo	-N-	BV Eri	-NN	V357 Peg	--N
VW Boo	-N-	FP Eri	--N	KN Per	--N
XY Boo	-N-	AK Her	-D-	V592 Per	--D
AC Boo	-N-	V829 Her	--D	VZ Psc	-N-
CK Boo	-C-	V972 Her	--N	AQ Psc	NNN
AO Cam	--D	FG Hya	N--	TY Pup	N--
DN Cam	--N	SW Lac	-DD	CW Sge	--D
BH CMi	--N	V407 Lac	--N	BE Scl	--C
V523 Cas	--N	UZ Leo	N--	RZ Tau	DDD
VW Cep	-D-	XY Leo	C--	EQ Tau	--N
TT Cet	NN-	XZ Leo	N--	V781 Tau	N-N
CL Cet	--N	AP Leo	N--	AG Vir	N--
CT Cet	--D	VZ Lib	-N-	AH Vir	D--
DY Cet	--N	UV Lyn	N--	GR Vir	-N-
RS Col	--N	V752 Mon	--D		

Notes.—The results are coded into three columns as follows: (hyphen) not observed in that run; (N) no detection; (D) detection at a separation of $<5''$; (C) a very close pair, with possible detection through a deformation of the diffraction pattern.

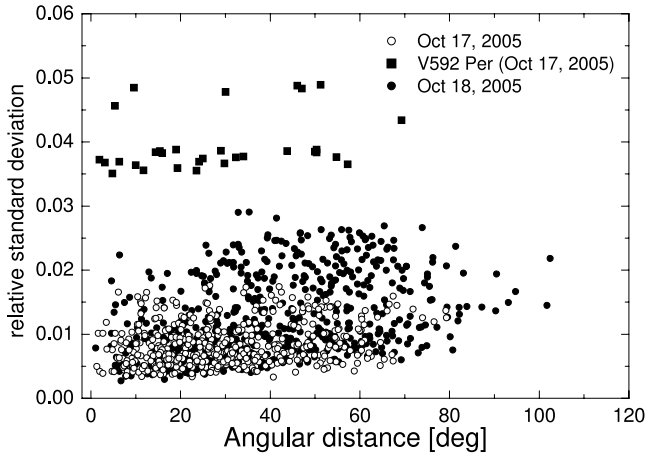

FIG. 1.—Similarity of the PSFs as a function of the angular distance on the sky. The relative standard deviation of mutual fits is for all possible pairs of stellar images. The images were matched within each night separately, as marked by different symbols. The system V592 Per stands out, as expected given that it has a very close, relatively bright companion.

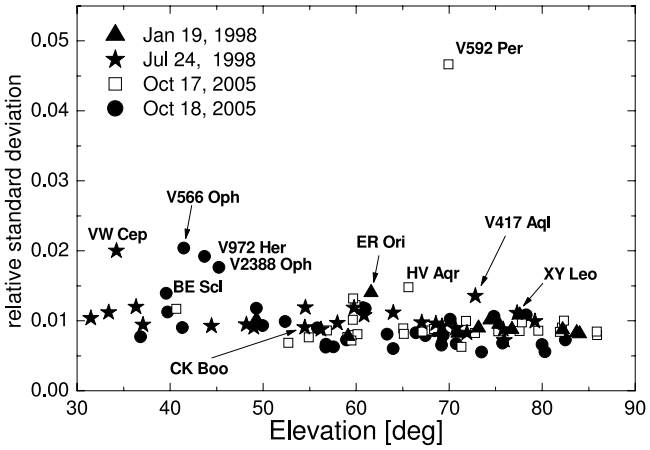

FIG. 2.—Similarity of the PSFs as a function of elevation. The relative standard deviation is computed for all templates used to fit the PSF of a given object. Objects showing large mismatches are suspected to have companions.

patch is relatively large, about 40″, and thus encompasses the whole field of view of the KIR camera. The Strehl ratio of the AO-corrected images was found to be almost constant (around 0.30) for all images taken in natural seeing better than 0.9″. On a few occasions of worse seeing, the Strehl ratio fell below 0.2. Although the amount of light scattered from the Airy disk into the rings increased on such occasions, the diffraction pattern was still very well defined. The measured FWHM of the AO-corrected images was 0.143″ in the *K* band, close to the expected diffraction-limited performance of a 3.6 m telescope.

The resulting point-spread function (PSF) of the corrected images is a combination of the diffraction pattern defined by the aperture of the telescope with a residual Gaussian and/or Lorenzian profile of much less understood character. Its shape was found to vary depending on the declination and the hour angle of the telescope (see § 3).

For the initial reductions we subtracted bias and dark current from the raw images, divided by flat fields, and removed hot pixels. Next we co-added all images for different sky displacements. For astrometry we measured the rotation and scaling of the AO system and its detector using known wide visual pairs with very slow orbital motion. The position angles for the 1998 and 2005 observing runs had to be corrected by -1° and $+4^\circ$, respectively, but no corrections to the pixel scale were needed. For both 1998 runs the correction was found to be the same.

3. DETECTION OF VISUAL COMPANIONS

In order to obtain maximum sensitivity to faint, close companions, we attempted to model the observed PSF of single targets. We first used an analytical combination of a Bessell function of the first order for the diffraction-limited part and a Gaussian function for the residual uncorrected light. The resulting representations turned out to be poor due to additional asymmetries in the PSF, visible as "gaps" at various position angles in the diffraction rings. Clearly, a heuristic approach was needed which would utilize the observed PSF shape as given by this particular combination of telescope, AO system, and camera.

Careful inspection of our images revealed that the PSF shapes were similar for most of the stars, but contained small residual deformations which depended primarily on the position of the telescope (Figs. 1 and 2) and, to a lesser degree, on the instantaneous seeing and the effective Strehl ratio of the corrected image.

To investigate the variation in the PSF shape, we fitted each stellar image to all images of other stars. While most systems showed just mild dependencies of the similarity in the image shape on various positional factors, some had systematically different shapes. We quantified the differences by a relative (to the maximum within the image) rms standard deviation of all fits to a given object using other images as templates. Some of the systems showing large mismatches are well-known close visual binaries where the secondary is located at a very small separation (VW Cep, V2388 Oph, ER Ori, and V592 Per), while some others were previously unrecognized as visual binaries (XY Leo and BE Scl). These results thus led to a cursory but rapid identification of close pairs.

Following this preparatory stage, we analyzed the images in more detail in two steps: (1) we determined the positions and magnitude differences of obvious and distant ($\rho > 1.0''$) companions from fluxes and centroid positions of their Airy disks (the mosaic of direct detections is presented in Fig. 3); and (2) we performed an automated search for faint companions which were missed in visual inspections or were too close to measure their positions and brightnesses. For the latter search we made direct fits to a binary model assuming that, within the isoplanatic patch, a binary can be represented by two properly shifted and scaled images of a well-chosen template. Thus, we express the observed image intensity for a visual double, $I(x, y)$, as

$$I(x,y) = B + A_1 T(x - x_1, y - y_1) + A_2 T(x - x_2, y - y_2), \quad (1)$$

where B is the background level, A_1 and A_2 are the normalization factors of the two stellar images (central star and companion, if present), $T(x, y)$ is the template image, and x_1, y_1 and x_2, y_2 are the spatial shifts of the template required to match the fitted images (for noninteger pixel shifts, we use bilinear interpolation in the template intensity). Thus, the fits involve three parameters entering linearly and four parameters entering nonlinearly. The performance of our technique is illustrated in Figure 4.9 for a very close companion to BE Scl.[4]

We found that the largest difficulty in identifying faint companions which might create only slight deformations of the PSF was to find a suitable template. To be as objective as possible, we

[4] Similar figures for eight additional systems, OO Aql, HV Aqr, CK Boo, VW Cep, XY Leo, V2388 Oph, ER Ori, and V592 Per, are also available in the electronic version (see Fig. Set 4).

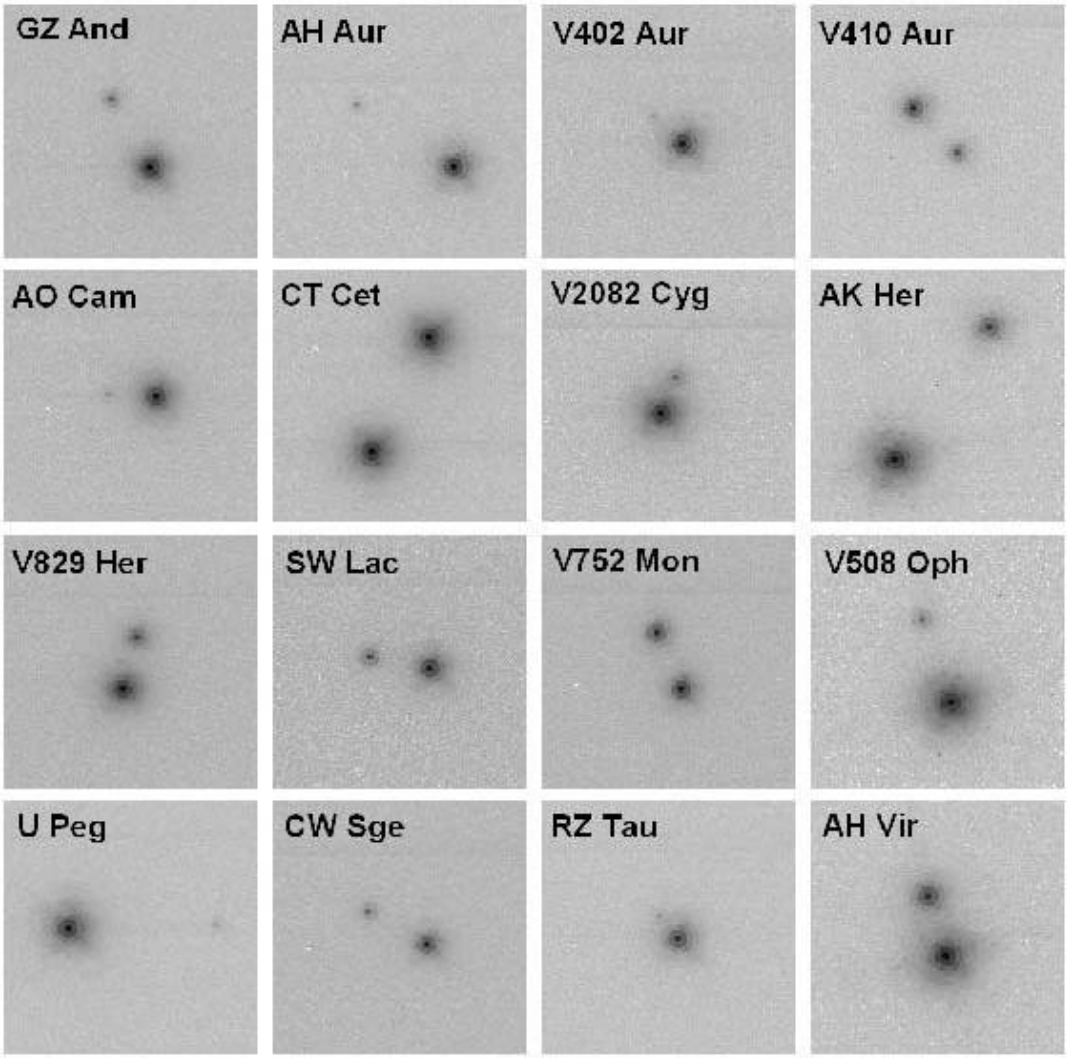

FIG. 3.—Mosaic showing systems for which the presence of a companion was obvious. The width of each panel corresponds to 7″.

performed an automated, brute-force search in which we fitted each object with a visual binary model which used, in succession, all other objects observed in a given run as templates (but omitting V592 Per and other objects already recognized as close pairs). To ensure that the fitting process did not converge only to local minima, and to increase the chance of finding real faint/close visual companions, we chose 24 initial positions for potential companions: eight different position angles θ, in steps of 45°, for three different initial separations ρ of 0.1″, 0.2″, and 0.3″ (i.e., sampling the region from the core to just outside the diffraction ring). As a starting magnitude difference, we used $\Delta M = 3$ mag. For a given object and a template combination, the fit with the best statistical quality, χ^2, from all possible starting sets of parameters was recorded. We rejected any fits that converged to separations closer than 0.02″.

Using as many templates as possible (e.g., 46 different stars for the 2005 observing run), we were able to assess the reliability of the detections and their significance level from the distribution of the recovered parameters. Also, with as many as 200 resulting parameter sets for a given object, we could reliably determine the final (mean) values and uncertainties for the various parameters for positive detections. For the 1998 runs we omitted a small number of *H*- and *K*-band observations and utilized only frames taken in the most frequently used filter, $K_{\rm CO}$.

One of the main difficulties in analyses like ours is to determine the significance of detections. We assessed it using the following scheme: For each successful convergence of the secondary position to a pixel inside an area of 100×100 pixels around the primary, we added a convergence unit "count" to that pixel, and we then looked in these "convergence maps" for count clustering. In other words, we took high numbers of counts for *all templates* as an indication of a distortion in the image which could be due to the presence of a companion. With this method, one immediately recovers close, but obvious, pairs for which almost all object-template fits lead to consistent sets of parameters. But one can also recover less obvious cases, as is illustrated in Figures 5.62 and 5.87,[5] where we show convergence maps for two systems, EQ Tau and BE Scl. Here EQ Tau is a typical case of no detection with a few spurious instances of the algorithm locking on small fluctuations within the first diffraction ring. However, for BE Scl one sees a clear clustering of successful convergences within a small circular area, indicating a genuine detection.

The approach described above has a limitation related to the increased random fluctuation noise in brighter portions of the image, particularly within the first ring, where the likelihood of the algorithm locking on random positive deviations is much larger.

[5] The convergence count maps for all objects are available in Figure Set 5.

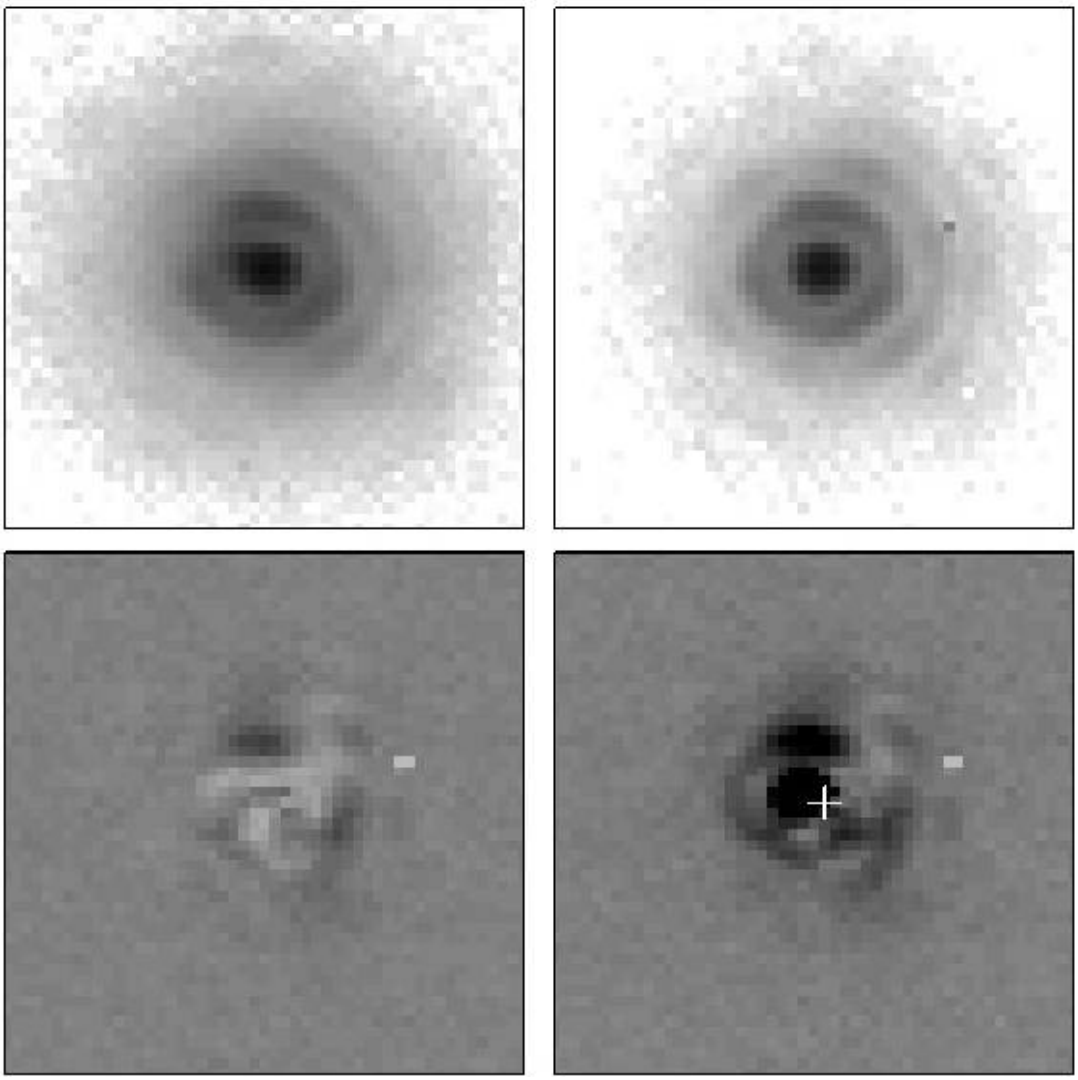

FIG. 4.9. Fitting a template to BE Scl.

FIG. SET 4.—Process of Fitting Model Binaries Using a Template. This example is for the very close visual binary BE Scl. The four panels show, clockwise from the top left, (1) the object image, (2) the template, (3) the secondary component (*white cross*) after subtraction of the primary, and (4) the residuals from the best fit. We used the five individual images (obtained by stacking several exposures at a given quadrant displacement) and fitted them with the best single exposures from 46 templates. Of the resulting 230 fits, 211 succeeded, while 19 did not; the figure shows one of the successful ones. The images are oriented with north up and east left. [Figs. 4.1–4.8 *for the eight remaining very close systems are available in the electronic version of the Astronomical Journal*.]

To assess the probability of false detections, we constructed a map similar to those we made for the individual stars, but obtained by adding the convergence maps for all stars which showed no indication of a companion (as for EQ Tau in Fig. 5.62). In practice, we added the low numbers of false detections in the diffraction rings for individual stars and obtained a "background map" of false detections against which our detections could be compared (Fig. 6). Note that we constructed these background images separately for the 1998 and 2005 runs; encouragingly, however, the images are very similar, indicating that the characteristics of the CFHT AO system did not change much between these two epochs.

With the convergence and background maps in hand, we assigned the significance of a detection using two approaches: (1) by simply taking the count maximum within the map or (2) by integrating (summing) the counts within a small (e.g., $r < 6$ pixels) aperture and comparing this with the number of counts in the same region in the background map. For both approaches, the relevant quantity required normalization by the number of object and template frames used. For each object and observing run, Table 3 gives the number of object frames, N_f, the number of templates used, N_t (28 in 1998 and 46 in 2005), and the number of frames used to construct the background map, N_b. For the first approach, the maximum number of counts within the count map (C) was then normalized to a typical number of object frames and templates of the 2005 run ($N_f = 5$, $N_t = 46$) as

$$C_n = C\frac{230}{N_f N_t}. \tag{2}$$

In the second approach, the sum of counts S in a cluster within a given aperture of radius r is divided by the corresponding summed count number (within the same area) in the background image B. The quality of the detection is then expressed as the normalized ratio of counts in the object and background maps:

$$R_n = \frac{S}{B}\frac{N_b}{N_f}. \tag{3}$$

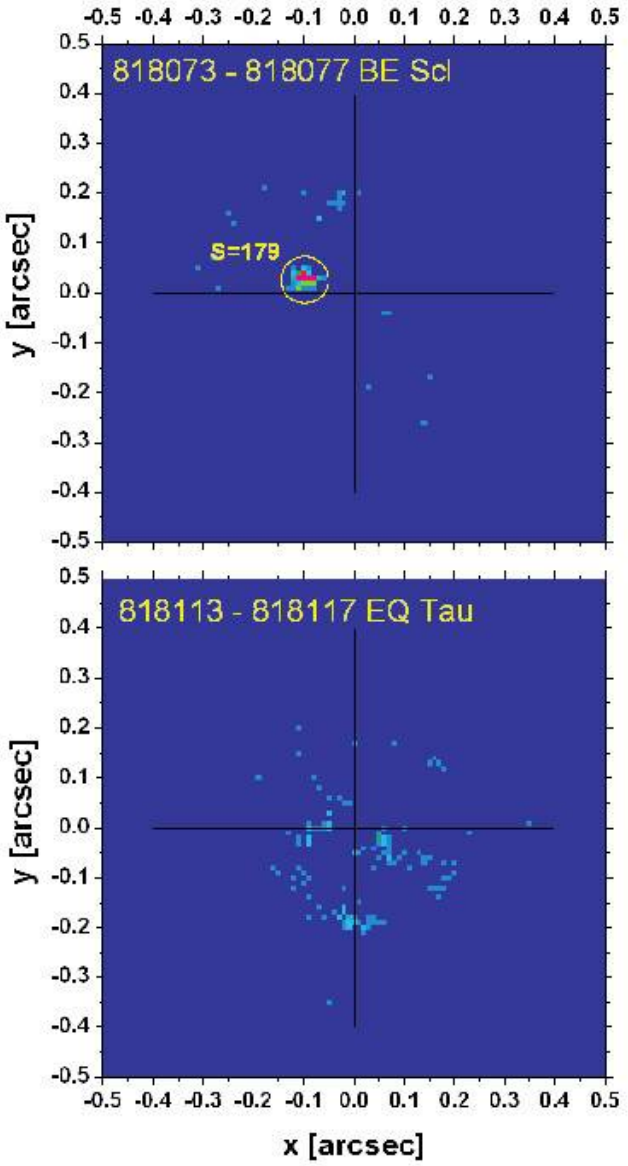

FIGS. 5.62 AND 5.87. Convergence count maps for BE Scl and EQ Tau.

FIG. SET 5.—Convergence Count Maps from the Automatic Search Routine. The 1998 observations were done in the CO filter, while the 2005 observations were done in the H_2 K-band filter. This example is for BE Scl and EQ Tau, the cases where images did not show any obvious evidence of a companion but the automatic search showed a clear detection for BE Scl, and no companion for EQ Tau. The total number per pixel is indicated by color. The circle for BE Scl encompasses a tight cluster of counts, in which 179 out of 211 of the fits indicated a companion could be present, indicating a real detection. No similar clustering is seen for EQ Tau. The maximum number of counts per pixel anywhere in the image is 4 for EQ Tau, but 52 for BE Scl. [Figs. 5.1–5.102 *are available in the electronic version of the Astronomical Journal*.]

In Table 3 we list the systems that show clustered counts within small circular apertures (with $r < 6$ pixels), and are thus suspected higher order systems, while in Table 4 we give maximum normalized counts C_n for systems for which no companions are suspected. Selection of a threshold for actual detection based on the "quantities of merit," C_n or R_n, was rather difficult and somewhat arbitrary; after some experiments, we felt the best distinction was achieved by taking as detections those objects that had $C_n > 20$ or $R_n > 50$, as listed in the last column of Table 3. With these thresholds, the automated search confirmed all suspected cases seen as deformation of the diffraction structure. These thresholds led to the confirmation of the four known tight pairs, V592 Per, VW Cep, ER Ori (1998 run), and V2388 Oph, and four new detections, HV Aqr (this one is also directly visible in the image), BE Scl, XY Leo, and CK Boo. Among these, XY Leo is the closest resolved system, with a separation of only 0.061″. The suspected cases, V376 And, TZ Boo, DN Cam, YY Eri, BV Eri, V829 Her, V508 Oph, V351 Peg, and TY Pup, clearly require new observations. The results for the automated search (presented in Tables 3 and 4) apply only for the detection of very close companions within 0.3″–0.4″. Hence, e.g., V829 Her having a distant companion clearly visible at 1.46″ is given as detection ("D") in Table 2, but there is only suspicion for a very close companion (Tables 3 and 4).

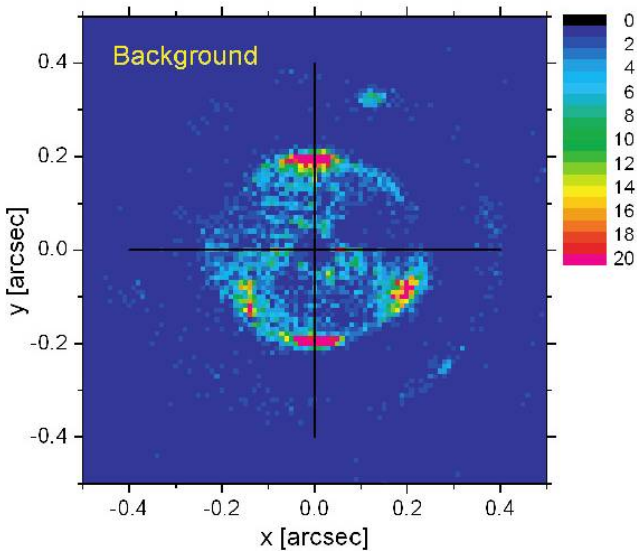

FIG. 6.—Background of false detections for all stars which do not show any visual companions (as observed in 2005; the 1998 images are very similar). The first diffraction ring and traces of the second ring are clearly visible.

The measured properties for the detected companions are given in Table 5. The table gives the designations of the components, the separation (ρ), the position angle (θ) in degrees, the magnitude differences in the K and H bandpasses, the Heliocentric Julian Date of the observation, and, from the date, the orbital phase of the binary and a correction of its brightness (see § 5). The table lists only systems with detected companions within 5″. Although this limit seems to be set arbitrarily, even faint companions separated by more than 5″ can be easily detected with small telescopes without AO. A good example is GZ And, where we give only our new detection at 2.13″; the components B and C, separated by 8.6″ and 13.3″, respectively, are clearly visible even in small telescopes (Walker 1973).

4. EVALUATION OF DETECTION LIMITS

The limit to which we were able to detect tertiaries for a given separation depended mainly on (1) the magnitude difference of the components in the K band, ΔK, and (2) the similarity of the PSFs for the object and the template. We assessed these limits by adding artificial stars to our real frames and applying the whole detection procedure.

We selected images of two single stars without any close ($\rho <$ 10″) companions, with AQ Psc serving as an object and FP Eri as a template. Artificial images were produced by shifting and

TABLE 3

Results of an Automated Search for Close Companions to Observed Contact Binaries: New Detections and Suspect Cases

Name	Year	N_f	N_t	N_b	C	C_n	r	S	B	R_n	Flag
V376 And	2005	10	46	268	11	5.5	4	46	84	14.7	S
HV Aqr	2005	5	46	268	51	51.0	4	141	4	1839.4	D
TZ Boo	1998	4	28	176	8	16.4	3	25	54	20.8	S
CK Boo	1998	8	28	176	13	13.3	5	103	15	155.7	D
DN Cam	2005	5	46	268	20	20.0	4	154	350	23.6	S
VW Cep	1998	4	28	176	63	129.4	3	107	4	1209.4	D
YY Eri	2005	5	46	268	9	9.0	4	80	830	5.2	S
BV Eri	2005	5	46	268	12	12.0	5	89	820	5.8	S
V829 Her	2005	5	46	268	11	11.0	6	144	597	12.9	S
XY Leo	1998	8	28	176	23	23.6	4	98	104	20.9	D
V508 Oph	1998	4	28	176	7	14.4	5	58	336	7.6	S
V2388 Oph	2005	5	46	268	21	21.0	4	144	109	70.8	D
ER Ori	1998	8	28	176	41	42.1	4	188	44	93.6	D
V351 Peg	2005	10	46	268	13	6.5	4	38	54	18.8	S
V592 Per	2005	5	46	268	134	134.0	4	221	62	192.2	D
TY Pup	1998	8	28	176	8	8.2	6	121	358	7.4	S
BE Scl	2005	10	46	268	93	46.5	4	372	127	78.4	D

Notes.—Explanation of columns: (name) variable star name in the General Catalog of Variable Stars; (year) year of the observing run; (N_f) number of object frames used for the count map; (N_t) number of templates used; (N_b) number of frames coming into the background map; (C) maximum count for the object; (C_n) normalized maximum count (see text for the definition); (r) radius of the aperture for the determination of the integrated counts in the object count map; (S) sum of counts within the selected aperture in the object map; (B) corresponding sum of counts in the background map; (R_n) normalized ratio of the summed counts in the object and the background map (see the text for the definition); (flag) status of the detection: (D) detection or (S) suspected case. The detection level is set at $C_n > 20$ or $R_n > 50$. Only detections with an automated search are taken into account; binaries with directly visible components are listed in Table 2 (see also Fig. 3).

co-adding the same object image for a wide range of separations ($0.04'' < \rho < 1.20''$) and magnitude differences ($0 < \Delta K < 6.5$ mag). For a given ΔK, the detection limit was determined as the minimum separation for which the algorithm would converge to the original position to within the FWHM of the PSF (we found our result was insensitive to the exact choice of convergence criterion). The resulting detection threshold curve, together with all actual detections, is displayed in Figure 7; its raggedness reflects the complex diffraction pattern in the PSF. This curve is very similar to curves published before for the same system (Duchêne et al. 1999; Bouvier et al. 2001). As one can see in Figure 7, the above criterion for the detection limit derived from artificial stars

TABLE 4

Results of an Automatic Search for Close Companions: Contact Binary Systems not Detected to Have Visual Companions

Name	Year	C_n	Name	Year	C_n	Name	Year	C_n
AB And	1998	6.2	DK Cyg	2005	2.0	V566 Oph	2005	7.0
AB And	2005	2.5	V401 Cyg	1998	8.2	V839 Oph	1998	14.4
GZ And	1998	2.1	V401 Cyg	2005	7.0	ER Ori	2005	4.5
GZ And	2005	9.0	V1073 Cyg	1998	12.3	V1363 Ori	2005	3.0
EL Aqr	1998	8.2	V1073 Cyg	2005	7.0	U Peg	1998	4.1
AH Aur	2005	4.0	V2082 Cyg	2005	3.0	U Peg	2005	2.0
V449 Aur	2005	10.0	LS Del	2005	4.0	BB Peg	2005	6.0
OO Aql	2005	4.0	SV Equ	1998	16.4	V335 Peg	2005	4.5
V417 Aql	1998	8.2	YY Eri	1998	6.2	V357 Peg	2005	4.0
V1464 Aql	2005	6.0	BV Eri	1998	2.1	KN Per	2005	6.0
V402 Aur	2005	1.5	FP Eri	2005	2.5	VZ Psc	1998	10.3
V410 Aur	2005	3.0	AK Her	1998	4.1	AQ Psc	1998	3.1
VW Boo	1998	2.1	V972 Her	2005	10.0	AQ Psc	1998	2.1
AC Boo	1998	4.1	SW Lac	1998	10.3	AQ Psc	2005	5.0
AO Cam	2005	7.0	SW Lac	2005	7.0	CW Sge	2005	4.0
BH CMi	2005	6.0	V407 Lac	2005	9.0	EQ Tau	2005	2.0
V523 Cas	2005	2.0	XZ Leo	1998	4.1	RZ Tau	1998	2.1
CL Cet	2005	4.5	AP Leo	1998	2.1	RZ Tau	2005	3.0
CT Cet	2005	9.0	VZ Lib	1998	4.1	V781 Tau	1998	3.1
DY Cet	2005	4.5	UV Lyn	1998	6.2	V781 Tau	2005	3.0
RS Col	2005	11.0	V752 Mon	2005	5.0	AG Vir	1998	2.1
RZ Com	1998	3.1	V753 Mon	2005	5.0	AH Vir	1998	6.2
SX Crv	1998	4.1	V502 Oph	1998	6.2	GR Vir	1998	3.1
CV Cyg	2005	2.0	V566 Oph	1998	10.3			

Notes.—Explanation of columns: (name) variable star name in the General Catalog of Variable Stars; (year) year of the observing run; (C_n) normalized maximum count (see text for the definition). Note that AQ Psc was observed in both 1998 January and July.

TABLE 5
COMPANIONS OF CONTACT BINARIES DETECTED OR CONFIRMED DURING THIS PROGRAM

Name	HJD (2,400,000+)	Phase	ΔV_ϕ	$\mu\Delta t$ (mas)	ρ (arcsec)	θ (deg)	ΔK	ΔH	M_K	M_H	Sp. Type
New Detections											
GZ And	51,019.1015	0.484	0.66	0.0	2.130(6)	33.55(7)	2.45(5)		5.99		M3 V
GZ And	51,019.1102	0.513	0.67	0.0	2.131(11)	33.51(10)		2.625(9)		6.24	M3–4
GZ And	53,660.9608	0.815	0.04	116.5	2.163(7)	29.25(13)	3.069(11)		5.99		M3 V
HV Aqr	53,660.7804	0.315	0.04	0.0	0.394(9)	12.4(8)	2.0(3)		4.3		K2–3 V
OO Aql	53,660.7339	0.835	0.16	0.0	0.510(16)	290(2)	5.1(3)		7.2		>M5 V
AH Aur	50,824.9048	0.072	0.29	0.0	3.189(4)	62.91(13)	4.31(4)		6.30		M5 V
AH Aur	50,824.9169	0.097	0.21	0.0	3.188(6)	62.98(18)		4.31(4)		6.26	M3–4 V
AH Aur	53,662.1136	0.170	0.06	154.0	3.159(4)	57.3(6)	4.74(5)		6.49		>M5 V
V402 Aur	53,661.0890	0.990	0.13	0.0	1.093(3)	47.1(3)	5.53(24)		7.00		>M5 V
V402 Aur	53,662.0200	0.533	0.12	0.0	1.093(3)	47.0(2)	5.29(3)		6.74		>M5 V
CK Boo	51,018.8040	0.351	0.08	0.0	0.12(4)	198(5)	2.8(9)		5.3		M1 V
AO Cam	53,662.0455	0.057	0.43	0.0	1.309(5)	87.87(15)	4.65(7)		7.68		>M5 V
V2082 Cyg	53,660.7223	0.927	0.06	0.0	1.049(4)	336.92(19)	3.12(4)		4.32		K2 V
V829 Her	53,661.7171	0.190	0.03	0.0	1.463(9)	344.69(22)	1.726(24)		4.07		K1 V
SW Lac	51,019.0182	0.825	0.10	0.0	1.680(1)	85.33(9)	2.554(9)		5.03		K9 V
SW Lac	51,019.0251	0.847	0.14	0.0	1.679(2)	85.36(19)		2.612(7)		5.19	K9 V
SW Lac	53,660.8173	0.004	0.84	642.3	1.680(4)	79.16(4)	1.86(3)		5.08		M0 V
XY Leo	50,825.0225	0.915	0.20	0.0	0.061(14)	91(7)	1.0(13)		4.7		K6 V
V508 Oph	51,018.9071	0.206	0.02	0.0	2.398(3)	18.85(5)	3.968(11)		6.50		>M5 V
V508 Oph	51,018.9152	0.229	0.00	0.0	2.395(3)	18.89(9)		4.275(11)		6.84	>M5 V
U Peg	51,019.0677	0.149	0.10	0.0	4.052(5)	275.38(9)	5.232(21)		7.78		>M5 V
U Peg	53,660.8890	0.206	0.02	515.0	4.076(5)	271.21(11)	5.60(5)		8.07		>M5 V
U Peg	53,661.8843	0.861	0.12	515.2	4.080(4)	271.25(11)	5.51(4)		8.09		>M5 V
CW Sge	53,660.7637	0.907	0.19	0.0	1.838(3)	60.68(17)	2.17(3)		3.51		G5 V
BE Scl	53,660.9444	0.059	0.33	0.0	0.102(19)	72(4)	1.4(7)		3.8		G8 V
BE Scl	53,661.9577	0.455	0.35	0.0	0.106(23)	74(4)	1.1(7)		3.4		G5 V
RZ Tau	50,824.8140	0.033	0.60	0.0	0.796(10)	43.76(10)	3.61(4)		6.23		M5 V
RZ Tau	50,824.8249	0.059	0.45	0.0	0.794(6)	43.7(4)		3.60(6)		6.10	M3 V
RZ Tau	51,019.1256	0.490	0.58	14.4	0.799(2)	44.02(11)	3.71(3)		6.31		>M5 V
RZ Tau	53,662.0090	0.503	0.58	210.5	0.801(4)	38.93(11)	4.29(5)		6.89		>M5 V
Confirmed Detections											
V410 Aur	53,661.0756	0.244	0.03	0.0	1.716(6)	224.59(10)	1.091(15)		3.52		K2 V
VW Cep	51,018.9527	0.326	0.06	0.0	0.254(8)	166.8(20)	1.4(2)				K4 V
CT Cet	53,661.9190	0.795	0.05	0.0	3.492(8)	206.73(8)	0.09(4)				G3 V
AK Her	51,018.8769	0.615	0.14	0.0	4.459(5)	324.37(7)	2.019(9)		4.13		K2 V
V752 Mon	53,661.1142	0.862	0.01	0.0	1.686(4)	23.89(15)	−0.50(2)				
V2388 Oph	53,661.7303	0.531	0.22	0.0	0.099(18)	31(13)	1.0(5)				F0 V
ER Ori	50,824.8540	0.197	0.03	0.0	0.178(14)	356(5)	2.0(4)				K2 V
ER Ori	53,661.1312	0.981	0.63	207.3							K2 V
V592 Per	53,661.0618	0.675		0.0	0.183(3)	207.9(14)	0.39(12)				G0:
AH Vir	50,825.1084	0.380	0.15	0.0	1.707(2)	16.50(7)	1.551(21)		3.98		K1 V

NOTES.—Explanation of columns: (name) variable star name in the General Catalog of Variable Stars; (HJD) Heliocentric Julian Date of the particular AO observation; (phase) orbital phase of the binary calculated from the ephemeris given below; (ΔV_ϕ) $V_{\rm obs} - V_{\rm max}$: correction required to bring the magnitude to the maximum visual brightness of the eclipsing pair for the instant of observation (see text); ($\mu\Delta t$) cumulative proper motion of the binary counted from the first observation (always 0 for stars observed during a single night); (ρ) angular separation of the components; (θ) position angle of the secondary (fainter) component; (ΔK, ΔH) measured magnitude differences between the visual companion and the binary (without correction for the phase of the eclipsing pair); (M_K, M_H) absolute magnitudes of the companion determined from the estimated absolute K and H magnitudes of the contact binary (Table 4), ΔK, ΔH, and ΔV_ϕ (see text); (sp. type) estimated spectral type of the visual companion. The ephemerides ($\rm HJD_{min} - 2{,}400{,}000 +$ period in days) used for the computation of the phases are as follows: (GZ And) 52,500.1198 + 0.3050177; (HV Aqr) 52,500.2163 + 0.3744582; (OO Aql) 52,500.261 + 0.5067932; (AH Aur) 52,500.3848 + 0.4941067; (V402 Aur) 52,500.567 + 0.60349867; (V410 Aur) 52,500.0033 + 0.3663562; (CK Boo) 52,500.026 + 0.3551538; (AO Cam) 52,500.1061 + 0.3299036; (VW Cep) 52,500.0321 + 0.2783108; (CT Cet) 48,500.1847 + 0.2564863; (V2082 Cyg) 52,466.1122 + 0.714084; (AK Her) 52,500.2709 + 0.421523; (V829 Her) 52,500.159 + 0.358153; (SW Lac) 52,500.1431 + 0.3207165; (XY Leo) 52,500.0872 + 0.2840978; (V752 Mon) 48,500.2837 + 0.462902; (V508 Oph) 52,500.0545 + 0.3447901; (V2388 Oph) 52,500.379 + 0.8022979; (ER Ori) 52,500.1715 + 0.4234018; (U Peg) 52,500.1288 + 0.3747766; (V592 Per) 53,399.3400 + 0.715722; (CW Sge) 52,500.567 + 0.6603631; (BE Scl) 52,500.0549 + 0.42290144; (RZ Tau) 52,500.3968 + 0.4156776; (AH Vir) 52,500.3174 + 0.407532.

is consistent with what we found from our automated search: all detected systems are above or at the detection limits.

5. NATURE OF THE COMPANIONS

We attempted to estimate the nature of the companions—assuming they are physically bound—from the measured brightness differences and estimates of the absolute magnitudes of the close binaries. The results are listed in Tables 5 and 6, with the former giving results for individual observations and the latter overall properties that we used or determined.

To obtain the best constraints on the companions, we first needed to ensure that our magnitude differences were evaluated relative

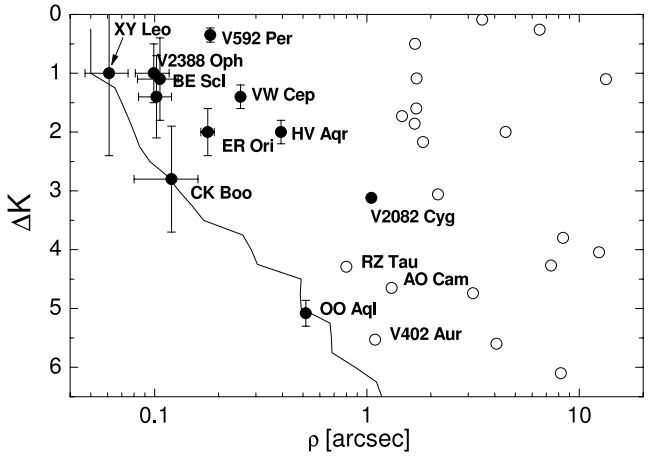

FIG. 7.—Detections of companions in our program as a function of the angular separation from the central star and the K magnitude difference. The detection limit evaluated by Monte Carlo experiments is shown by the solid curve. Detections resulting from our automated search and modeling are shown by filled circles, while wider pairs for which the measurement of the components was done separately are shown by open circles. Of the three sources near the detection limit, the detection of the faint companion to OO Aql is unambiguous, but the cases of CK Boo and XY Leo require confirmation (see § 7 for details).

to the maximum brightness of the contact binary. This is important for some contact binaries showing large photometric amplitudes (e.g., GZ And, OO Aql, SW Lac, ER Ori, and U Peg with $\Delta V > 0.70$ mag). Thus, knowledge of the orbital phase is necessary for a proper estimate of the instantaneous brightness of the contact binary. The phases at the time of the AO observations were calculated using the Cracow online, up-to-date ephemeris database[6] (Kreiner et al. 2001; Kreiner 2004). The visual magnitude of the contact binary was then estimated by using published light curves (sometimes by graphical tracing in figures) to determine the difference from the maximum brightness $V_{\max}$ (the latter was usually taken from the General Catalogue of Variable Stars[7]).

To convert these V magnitudes at the time of observation to absolute magnitudes M_V, we used *Hipparcos* parallaxes with relative precision better than 15% if available (an error of <0.30 mag in the absolute magnitude) and the period-color-luminosity relation of Rucinski & Duerbeck (1997; an error of ~ 0.30 mag) for systems with poorer parallaxes (GZ And, V829 Her, OO Aql, AO Cam, and ER Ori). Because all objects are nearby, we neglected interstellar absorption.

Next, to calculate expected absolute magnitudes M_K at the time of observation, we used MS colors appropriate for the spectral types of the binaries (as determined from DDO observations; see Pribulla et al. [2006, 2007] for references to previous publications). Here we note that in comparing contact binaries with single stars, one must take into account that while they are MS objects, the energy transfer from the primary to the secondary component makes the primary component always cooler than a MS star of the same mass (Mochnacki 1981). Furthermore, because of the increased radiating area, the absolute visual magnitude M_V of a contact binary obtained directly from its trigonometric parallax and $V_{\max}$ is always brighter than the M_V corresponding to a single MS star of the same spectral type. However, for a given spectral type contact binaries appear to have the same colors (S. M. Rucinski, unpublished comparison of $B-V$ and $V-K$ indices), so that our simple corrections are adequate to evaluate M_K.

Finally, with M_K for the contact binary at the time of the observation, the observed magnitude difference then yields the absolute magnitude of the companion, and, with the appropriate MS relations, the estimated spectral type. One sees that most of the companions appear to be late, M0–M6 dwarfs, with some, such as those of U Peg and V402 Aur, of even later spectral types.

To estimate the orbital periods of wide visual orbits of triple systems, we also calculated the total masses of the contact binaries by combining radial-velocity orbits such as those obtained at DDO (Pribulla et al. 2006, 2007), which give $(M_1 + M_2)\sin^3 i$, with photometric observations, which provide the orbital inclination i. In the selection of such combined solutions, we preferred the total masses determined by simultaneous light and radial-velocity curve fits (Gazeas et al. 2006). The total masses of the systems (using the estimated mass of the third companion) were then used to estimate an approximate orbital period of the visual pair from the angular separation and the distance.

6. THE PHYSICAL BOND

While the presence of a star close to several contact binaries is unquestionable, the physical link is often difficult to prove. There are three possible ways of assessing the physical bond:

Observed color difference.—With observations in multiple photometric bands, one can verify that the spectral type of the companion inferred from its magnitude—assuming the same distance as the contact binary—is consistent with its colors. Unfortunately, we can do this for only a few systems, since most of the data were obtained in one passband (K and its narrowband substitute). Moreover, even for systems observed in H and K, the constraint is weak, since the $(H-K)$ color index is insensitive to the spectral type (Cox 2000): for most MS stars, it is in the range $-0.04 < H-K < 0.11$ and starts increasing to $\simeq 0.33$ only at spectral types of about M5 V. We find that in our current sample, the available color indices usually agree moderately well with the absolute K-band magnitudes of the companions (see § 7). For future confirmations, a more suitable index would be the $(J-K)$ color index, which increases monotonically from -0.22 at O5 to 0.86 at M2, then becomes nearly constant in M dwarfs, then increases strongly again for L dwarfs. A disadvantage of using $(J-K)$, however, is that the performance of AO systems is substantially worse in the J passband.

For some binaries we can compare the infrared magnitude differences with the visual flux ratio $L_3/(L_1+L_2)$ obtained from the averaged spectra. This gives a much larger wavelength base, but works only in cases when the third component was located well within the spectrograph slit. For consistency, the visual flux ratio should be measured relative to the maximum light of the contact binary.

Similarity of the proper motion.—For systems where the contact binary has a relatively high proper motion, say $\mu = (\mu_\alpha^2 \cos^2\delta + \mu_\delta^2)^{1/2} > 50$ mas yr^{-1}, an *optical* companion would show an optical projection motion between our 1998 and 2005 observing runs, while a physically bound one would not (provided the orbital period is sufficiently long that no orbital motion is expected). To test this, we collected proper motions (Table 6) from the Tycho-2 catalog (Høg et al. 2000) for all systems except GZ And (which was not observed, and for which we adapted the proper motion from the Second USNO CCCD Astrograph Catalog; Zacharias et al. 2004). We found that the companions to the large proper motion contact binaries AH Aur, SW Lac, U Peg, and RZ Tau had the same relative position in both the 1998 and

[6] See http://www.as.ap.krakow.pl/ephem/.

[7] We used the most recent electronic version (4.2), available at http://www.sai.msu.su/groups/cluster/gcvs/.

TABLE 6

PROPERTIES OF CONTACT BINARIES WITH NEWLY DETECTED COMPANIONS

Name	V_{max}	ΔV	π (mas)	σ_π (mas)	μ (mas yr^{-1})	Sp. Type (1,2)	$(B-V)_0$	M_V Calc.	M_V Spec.	M_H Spec.	M_K Spec.	M_H Corr.	M_K Corr.	M_{12} ($M_\odot$)	Sp. Type Comp.	M_3 ($M_\odot$)	a (AU)	P_{vis} (yr)
GZ And	10.83	0.78	5.33	...	16.1	G5 V	0.68	4.46	5.10	3.52	3.58	2.94	2.88	1.708	M3–4 V	0.3	400	5500
HV Aqr	9.71	0.40	5.33	...	112.0	F5 V	0.44	3.34	3.50	2.40	2.44	2.28	2.24	1.569	K2–3 V	0.7	74	430
OO Aql	9.20	0.80	7.19	...	66.2	G5 V	0.68	3.48	5.10	3.52	3.58	1.96	1.90	1.954	>M5 V	<0.2	71	420
AH Aur	10.20	0.37	6.18	2.05	19.8	F7 V	0.49	2.96	3.83	2.57	2.61	1.74	1.70	1.967	M5 V	0.2	510	8200
V402 Aur	8.84	0.14	7.01	1.31	11.3	F2 V	0.35	2.15	3.60	2.78	2.82	1.37	1.33	1.965	>M5 V	<0.2	156	1370
CK Boo	8.99	0.27	6.38	1.34	111.9	F7.5 V	0.51	3.66	3.92	2.61	2.64	2.37	2.35	1.569	M1 V	0.45	19	54
AO Cam	9.50	0.50	7.98	...	0.0	G0 V	0.58	4.01	4.40	2.99	3.04	2.65	2.60	1.605	>M5 V	<0.2	164	1630
V2082 Cyg	6.63	0.05	11.04	0.56	97.0	F0 V	0.30	1.84	2.70	2.00	2.03	1.17	1.14	...	K2 V	0.75	95	...
V829 Her	10.10	0.29	4.97	...	19.6	F7 V	0.49	3.58	3.83	2.57	2.61	2.36	2.32	1.806	K1 V	0.77	295	3570
SW Lac	8.51	0.88	12.30	1.26	88.8	G5 V	0.68	3.96	5.10	3.52	3.58	2.44	2.38	2.204	K9 V	0.54	136	940
XY Leo	9.45	0.48	15.86	1.80	81.3	K0 V	0.81	5.45	5.90	3.94	4.02	3.57	3.49	1.188	K6 V	0.64	3.8	5.5
V508 Oph	10.06	0.63	7.68	2.14	47.4	G0 V	0.58	3.92	4.40	2.99	3.04	2.56	2.51	1.520	>M5 V	<0.2	310	4400
U Peg	9.23	0.84	7.18	1.43	71.2	G2 V	0.63	3.92	4.70	3.24	3.29	2.51	2.46	1.554	>M5 V	<0.2	560	10600
CW Sge	11.13	0.80	2.57	4.14	2.1	F5 V	0.44	2.25	3.50	2.40	2.44	1.19	1.15	...	G5 V	0.92	715	...
BE Scl	10.24	0.43	9.76	5.11	19.5	F8 V	0.52	3.35	4.00	2.65	2.70	2.05	2.00	...	G5–8 V	0.8–0.9	10	...
RZ Tau	10.08	0.63	5.74	1.85	27.1	F0 V	0.30	2.72	2.70	2.00	2.03	2.05	2.02	...	>M5 V	<0.2	139	...

NOTES.—Explanation of columns: (name) variable star name in the General Catalog of Variable Stars; (V_{max}) Johnson or transformed *Hipparcos* H_p maximum light magnitude; (ΔV) amplitude of the light variations; (π, σ_π) trigonometric parallax and its error (if given without error, photometrically determined parallax; see text); (μ) proper motion: $\mu = [(\mu_\alpha \cos\delta)^2 + (\mu_\delta)^2]^{1/2}$; [sp. type (1,2)] spectral type of the binary; [$(B-V)_0$] dereddened color index; (M_V calc.) absolute visual magnitude calculated from V_{max} and the *Hipparcos* parallax (for V2082 Cyg, SW Lac, and XY Leo) or from the Rucinski & Duerbeck (1997) calibration; ($M_{V,H,K}$ spec.) absolute V, H, and K magnitudes corresponding to a MS star of the same spectral type as the contact binary; ($M_{H,K}$ corr.) corrected absolute magnitudes of the contact pair (see text); (M_{12}) total (not projected, sin i accounted for) mass of the contact binary; (sp. type comp.) estimated spectral type of the visual companion; (M_3) estimated mass of the visual companion (according to the tabulation in Cox 2000)]; (a) projected separation determined from angular separation and distance; (P_{vis}) estimated period of the visual orbit.

the 2005 runs, and therefore, for all four cases we thus are virtually certain that the companions are physical ones.

Among the systems observed only on one occasion, there are a few further ones with large proper motions for which the test should be feasible in a few years. These are HV Aqr, V508 Oph, CK Boo, and V2082 Cyg (see Table 6).

Similarity in radial velocities.—Another kinematical indicator of physical association is a similarity of the center-of-mass radial velocity of the contact binary and of the radial velocity of the companion, a condition which should be valid for companions on long-period orbits. Indeed, several companions detected within the current program (GZ And, HV Aqr, CK Boo, AO Cam, and V2082 Cyg), independently found from the analysis of the averaged spectra from DDO in Paper II, show radial velocity consistent with the systemic velocity of the contact binary.

7. RESULTS FOR INDIVIDUAL SYSTEMS

We give summaries of the properties of the contact binaries with newly detected companions in Table 6. Here we discuss some of the new detections, as well as systems with interesting nondetections. The WDS numbers below refer to entries in the Washington Double Star Catalog (Mason et al. 2001).

GZ And.—A new component found in the trapezoidal multiple system GZ And (WDS J02122+4440) is very probably a physical member: the estimated M_K indicates a spectral type of M5 V or later, and this is supported by its color, $(H - K) = 0.25$, which is appropriate for an M3–4 dwarf.

HV Aqr.—Indications of a faint tertiary to HV Aqr were first found in Paper II, with an estimated light contribution at 5184 Å of $L_3/(L_1 + L_2) \approx 0.022$ ($\Delta V = 4.14$ mag) and a companion temperature of $T_3 \simeq 4000$ K. This is consistent with the infrared AO observations, which give $\Delta K = 2.00$ mag and from which we inferred F0 and K5 spectral types.

AH Aur.—Although the visual companion to AH Aur is relatively distant, at 3.16″, the proper motion indicates a physical association: if the visual companion is a distant background star, the relative position of components should have changed by ∼0.15″ between the two epochs of our observations, but it has been found to be stable within 0.02″.

CK Boo.—A late-type companion to CK Boo was first found in Paper II, with $L_3/(L_1 + L_2) = 0.009$ ($\Delta V = 5.11$) and $T_3 \simeq$ 3900 K. This is consistent with what is expected for the M0 V dwarf inferred from our AO observations. The detection in our automated search seems to be particularly reliable because the component appears in a practically empty part of the background count map.

VW Cep.—The companion to VW Cep (WDS J20374+7536) was discovered by Heintz (1974). The last published astrometric observation in the WDS is from 1999 with $\rho = 0.4''$ and $\theta = 187^\circ$. Our position, $\rho = 0.254''$ and $\theta = 167^\circ$, is closer to the periastron passage, which occurred in 1997 January and is consistent with the position at $\rho = 0.249''$ and $\theta = 165.2^\circ$ expected from the elements in the Sixth Catalog of Orbits of Visual Binary Stars (see Hartkopf et al. 2001). Since there appear to be no other observations close to periastron, our new position has the potential to markedly improve the companion orbit.

CV Cyg.—From *Hipparcos* measurements, it was found that CV Cyg (WDS J19543+3803) consisted of two almost identical stars separated by $\rho = 0.7''$ at $\theta = 140^\circ$ and $\Delta V = 0.02$. Surprisingly, however, our observations do not show any indications of a companion. Furthermore, the photometric study of Vinkó et al. (1996) found no evidence for any third light in the system, and a single spectrum of Hα taken by Vinkó et al. does not show any indication of ternarity. We thus suspect that the *Hipparcos* discovery is spurious.

V2082 Cyg.—A late-type companion to V2082 Cyg, with a light contribution of $L_3/(L_1 + L_2) \approx 0.02$ and a temperature $T_3 \simeq$ 5100 K, was found in Paper II. Independently, in Paper I we found an indication for a late-type tertiary from the relatively high X-ray–to–bolometric flux ratio, which was unexpected for the binary itself, since it has a moderately long orbital period, $P = 0.714$ days, and an early spectral type, F0 (Pych et al. 2004). At $\rho = 1.05''$ the system is very probably physically bound. The visual and infrared magnitudes are consistent with a companion of the K2/3 V spectral type.

V829 Her.—The possible multiplicity of V829 Her was indicated by a large proper-motion error and an acceptable light-time effect (LITE) solution for the contact binary (Paper I). If one uses the photometrically estimated parallax of Bilir et al. (2005), 13.53 ± 0.54 mas, with the LITE-derived $a_{12} \sin i = 0.9 \pm 0.2$ AU and assumes the masses of the components from Paper I the angular separation should be about 0.08″. Thus, it is clear that the observed LITE cannot be caused by the object we detected at $\rho = 1.46''$. If both the LITE and AO companions are confirmed, the system will be part of a quadruple system.

SW Lac.—Indications for the multiplicity of SW Lac have been found both from spectra, which show a late-type contribution (Hendry & Mochnacki 1998), and from complicated changes of its orbital period (Pribulla et al. 1999). Our AO observations show a relatively distant companion, at a separation of 1.68″. Its physical bond to the contact binary is practically certain, as SW Lac moved by 0.64″ on the sky between 1998 and 2005 due to the fast proper motion, while the relative position of the visual components has remained stable to within 0.01″. The colors of the companion, $(H - K) = 0.11$–0.16, correspond to a K5–M1 V dwarf, which is consistent with the late-K dwarf inferred from the K-band magnitudes. This visual companion might, despite the large separation, be responsible for the spectral signature but cannot be responsible for the observed LITE. Thus, another companion could be hiding at a still smaller separation.

XY Leo.—The multiple nature of XY Leo was first indicated by the LITE, and the interpretation and expected nature of the third body were extensively discussed by Gehlich et al. (1972). Barden (1987) found spectroscopically that the companion was a BY Dra binary of a mid-M spectral type with a short orbital period of 0.805 days. Thus, the system is a quadruple consisting of two close binaries. From the mass function of the third component determined from the LITE orbit, Barden (1987) estimated that the orbital inclination of the outer orbit must be close to 90°. The visual pair has not yet been resolved directly. If our marginal detection (§ 3) is confirmed, then, when combined with the LITE parameters of Paper I, the inclination of the outer orbit should be about 67°, with a longitude of the ascending node of about 22° (or 202°). The largest separation of ≈0.17″ appears to have occurred in the summer of 2003. In 2013 occurs the second maximum at a separation of 0.13″. Two or three spectroscopic runs within the orbital period of the outer binary of 20 years would be needed to lift the ±180° ambiguity in the orientation of the orbit (Ω) and to estimate the total mass of the whole quadruple system.

V508 Oph.—The multiplicity of V508 Oph was first indicated by *Hipparcos* astrometry, with the system having an "S" flag in the H61 field. The estimated color of the visual companion to V508 Oph, $(H - K) = 0.34$, indicates an M5 V dwarf, consistent with the inferred absolute magnitude.

V2388 Oph.—V2388 Oph (WDS J17543+1108) is a known close visual pair on an 8.92 yr orbit with one component being an eclipsing binary. The separation of the components is only about

0.09″, and the system has been the subject of many speckle interferometry observations. The visual magnitude difference of components was determined spectroscopically to be $L_3/(L_1 + L_2) = 0.20 \pm 0.02$, corresponding to $\Delta V = 1.75 \pm 0.02$ mag (Rucinski et al. 2002). Given the F2 V classification of V2388 Oph, the observed ΔV implies a G5 spectral type for the companion. Thus, one expects $\Delta K \approx 0.8$, which is consistent with what we find. Oddly, however, the position predicted by elements in the Sixth Catalog of Orbits of Visual Binary Stars (Hartkopf et al. 2001), $\rho = 0.075''$ and $\theta = 203^\circ$, is inconsistent with our observation. Our measured $\theta = 31^\circ \pm 13^\circ$ suggests the components were swapped in the Sixth Catalog.

ER Ori.—The visual companion to ER Ori (WDS J05112−0833), at $\rho = 0.187''$, $\theta = 354.4^\circ$, and $\Delta V = 2.0$ mag, was first noticed in observations in 1993 March by Goecking et al. (1994). In our 1998 January observations we find the companion at practically the same position ($\rho = 0.183''$, $\theta = 354.4^\circ$, and $\Delta K = 2.14$ mag), but curiously, in our 2005 October observations there is no trace of it. Given the excellent detection quality, the companion is almost certainly real, and almost certainly physically associated with the contact binary. We note that the proper motion of the contact binary is directed to the south, while the companion was observed to the north of the contact binary in 1993 and 1998; thus, if the stars are unrelated, the separation should have increased.

The presence of a companion to the binary is also indicated by two other effects. First, there are large acceleration terms in the *Hipparcos* astrometric solution, $g_\alpha = -19.26 \pm 6.57$ mas yr^{-2} and $g_\delta = -17.34 \pm 4.71$ mas yr^{-2}, which suggests an orbital period of only a few years. Second, the arrival times of the ER Ori eclipsing system clearly show the LITE, with an implied outer orbit with a period of about 50 yr (Kim et al. 2003), a semimajor axis for the eclipsing pair of 6.7 AU, and a substantial eccentricity, $e = 0.89$. From this orbit, periastron passage was predicted around 2004 July/August, and this might explain the absence of the visual companion during the CFHT 2005 observing run.

U Peg.—Although the visual companion to U Peg is rather faint and distant, the fast proper motion of the contact binary, amounting to 0.515″ between the 1998 and 2005 runs, has helped confirm the physical association: the relative position of the components remained stable within 0.03″.

V592 Per.—This binary (WDS J04445+3953) has a known close visual companion that shows a slow orbital motion. According to the WDS, between 1977 and 2003 the P.A. changed from $\theta = 190$ to 209°. Our P.A., $207^\circ \pm 2^\circ$, is consistent with the most recent published observation in the WDS. The magnitude difference of the components as given in the WDS is $\Delta V = 0.85$. From our AO observations, we derive $\Delta K = 0.39 \pm 0.06$, which is fairly consistent with the estimated spectral type of the contact binary (F5–6; see Rucinski et al. 2005) and a G0 V spectral type for the visual companion. The components have very similar radial velocities (Rucinski et al. 2005).

CW Sge.—The binary was suspected to be a member of a short-period visual pair because it is flagged by "X" (stochastic astrometric solution) in the H59 *Hipparcos* catalog field (Paper I). This resulted in a *Hipparcos* parallax with a large error, $\pi = 2.57 \pm 4.14$ mas. The *Hipparcos* so-called cosmic error, $\epsilon = 7.64 \pm 1.32$ mas, suggests a rather small size for the astrometric orbit. The companion detected by our AO observations at a separation of 1.84″ cannot be identified with the one causing the rapid astrometric motion. Therefore, CW Sge may be a member of a system with higher multiplicity.

BE Scl.—The multiplicity of BE Scl was indicated by the large "cosmic error," $\epsilon = 13.36 \pm 1.35$ mas, in its *Hipparcos* astrometric solution. Our analysis shows a close companion at $\rho = 0.1''$ with $\Delta K = 1.1. . .1.4$. This companion is likely responsible for the observed astrometric motion. With a large photometric amplitude of about 0.45 mag, the eclipsing pair is an easy object for timing of the eclipses and is expected to show variations on timescales shorter than 1 yr.

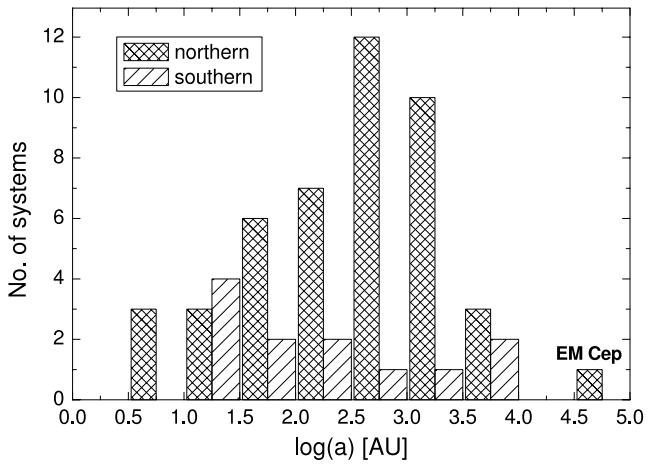

FIG. 8.—Distributions of projected separations (in AU) for resolved systems brighter than $V_{max} = 10$. This figure is an update of Fig. 9 in Paper I. The distributions are shown separately for both hemispheres (relative to the equator), since the northern hemisphere has been better studied. The six new systems, OO Aql, HV Aqr, V402 Aur, AO Cam, V2082 Cyg, and XY Leo, are all located in bins with $0.5 < \log a(\mathrm{AU}) < 2.0$.

RZ Tau.—The possible multiplicity of RZ Tau was first indicated by *Hipparcos* astrometry, with RZ Tau having an "S" flag in the H61 field. The physical association of the visual pair is supported by a stable relative position of its component between the 1998 and 2005 observations, despite the fact that the proper motion of the contact binary caused it to move 0.21″ on the sky.

8. SUMMARY

We present the results of an AO search for companions of contact binary stars conducted on four nights in 1998 and 2005, in an attempt to confirm their high apparent incidence indicated by various approaches in Paper I. The preliminary results of the 1998 observations were included in Papers I and II; the new observations, taken in 2005, have contributed six additional companions to the magnitude-limited sample ($V_{max} = 10$). The 2005 observations covered the fall part of the CFHT sky and were much more consistent in terms of the object selection than the 1998 observations. Figure 8 gives the updated distribution of projected separations for all objects in our program. Our new discoveries fall into the range of relatively small separations within $0.5 < \log a(\mathrm{AU}) < 2.0$.

For separations larger than 1″, the companions were easily visible in the images, but for subarcsecond detections we relied on an automated search technique which was able to find companions hiding within the AO diffraction rings. This new technique permitted us to approach the effective resolution limit of the CFHT AO system of about 0.07″–0.08″ in the K band. The main results are shown in Figure 7 and are listed in Table 5. Thanks to this new technique we were able to detect very close companions to XY Leo, V2388 Oph, and BE Scl, while for nine additional systems very close companions are suspected; these systems require further observations. Especially encouraging are the AO detections of companions previously indicated by other techniques in Papers I and II (e.g., OO Aql, V2082 Cyg, V829 Her, CW Sge, and BE Scl). We note that contact binaries with

third components with $\rho < 1''$ are perfect objects for tests of ground-based interferometric system imaging because a companion can provide an ideal phase reference source.

From our detection limits shown in Figure 7, we can evaluate our selection biases and estimate how many systems might have been missed by our AO observations at large magnitude differences ΔK and small separations ρ. From this figure one sees that the distribution of companions as a function of magnitude difference is rather flat at large separations, $\rho > 1''$. Similarly, for relatively bright companions one sees that the distribution in $\log \rho$ is relatively flat. If the two distributions are independent, then this suggests that in addition to the 11 systems at subarcsecond separations that we detected, another 11 or so may have fallen below our separation detection limit (to $\Delta K \simeq 6$). If we corrected our results for those presumably missed companions, the implied incidence would increase from $31\% \pm 6\%$ (25 detections in a sample of 80 contact binaries) to $45\% \pm 8\%$.

By combining the current results for the actual detections for binaries with $V_{\max} < 10$ with our earlier AO detections reported in Paper I, we obtain the total fractional incidence of triple systems of $61\% \pm 8\%$ for northern objects and $19\% \pm 5\%$ for southern objects, strengthening the hypothesis that all close binaries are members of multiple systems. Finally, we note that from the 151 known contact binaries brighter than $V_{\max} = 10$ mag, so far only 51 have been observed with an AO system. Extrapolating the detection rate from the present sample, one would expect some 30 new AO detections or confirmations (of the cases listed in Paper I) for the 100 binaries which remain to be observed with the AO technique. For the reason that about two-thirds of all systems still remain to be observed, we defer a detailed comparison of the current results with the statistics of the solar-type field stars of Duquennoy & Mayor (1991) until such a full sample becomes available.

The research made use of the SIMBAD database, operated at the CDS, Strasbourg, France, and accessible through the Canadian Astronomy Data Centre, which is operated by the Herzberg Institute of Astrophysics, National Research Council of Canada. This research made also use of the Washington Double Star Catalog maintained at the US Naval Observatory. Support from the Natural Sciences and Engineering Council of Canada (NSERC) to S. M. R. and M. H. v. K. is acknowledged with gratitude; visits of T. P. to the University of Toronto were supported by the NSERC grant of S. M. R.

REFERENCES

Barden, S. C. 1987, ApJ, 317, 333
Bilir, S., Karatas, Y., Demircan, O., & Eker, Z. 2005, MNRAS, 357, 497
Bouvier, J., Duchêne, G., Mermilliod, J.-C., & Simon, T. 2001, A&A, 375, 989
Cox, A. N. 2000, Allen's Astrophysical Quantities (New York: Springer)
D'Angelo, C., van Kerkwijk, M. H., & Rucinski, S. M. 2006, AJ, 132, 650 (Paper II)
Duchêne, G., Bouvier, J., & Simon, T. 1999, A&A, 343, 831
Duquennoy, A., & Mayor, M. 1991, A&A, 248, 485
Gazeas, K. D., Niarchos, P. G., Zola, S., Kreiner, J. M., & Rucinski, S. M. 2006, Acta Astron., 56, 127
Gehlich, U. K., Prölss, J., & Wehmeyer, R. 1972, A&A, 18, 477
Goecking, K.-D., Duerbeck, H. W., Plewa, T., Kaluzny, J., Schertl, D., Weigelt, G., & Flin, P. 1994, A&A, 289, 827
Hartkopf, W. I., Mason, B. D., & Worley, C. E. 2001, AJ, 122, 3472
Heintz, W. D. 1974, IAU Circ. 2698
Hendry, P. D., & Mochnacki, S. W. 1998, ApJ, 504, 978
Høg, E., et al. 2000, A&A, 355, L27
Kim, C.-H., Lee, J. W., Kim, H. I., Kyung, J. M., & Koch, R. H. 2003, AJ, 126, 1555
Kreiner, J. M. 2004, Acta Astron., 54, 207
Kreiner, J. M., Kim, C. H., & Nha, I. S. 2001, An Atlas of ($O-C$) Diagrams of Eclipsing Binary Stars (Kraków: Wyd. Nauk. Akad. Ped.)
Mason, B. D., Wycoff, G. L., Hartkopf, W. I., Douglass, G. G., & Worley, C. E. 2001, AJ, 122, 3466 (WDS)
Mochnacki, S. W. 1981, ApJ, 245, 650
Pribulla, T., Chochol, D., & Parimucha, Š. 1999, Contrib. Astron. Obs. Skalnaté Pleso, 29, 111
Pribulla, T., & Rucinski, S. M. 2006, AJ, 131, 2986 (Paper I)
Pribulla, T., Rucinski, S. M., Conidis, G., DeBond, H., Thomson, J. R., Gazeas, K., & Ogłoza, W. 2007, AJ, 133, 1977
Pribulla, T., et al. 2006, AJ, 132, 769
Pych, W., et al. 2004, AJ, 127, 1712
Rigaut, F., et al. 1998, PASP, 110, 152
Rucinski, S. M., & Duerbeck, H. W. 1997, PASP, 109, 1340
Rucinski, S. M., Lu, W., Capobianco, C. C., Mochnacki, S. W., Blake, R. M., Thomson, J. R., Ogłoza, W., & Stachowski, G. 2002, AJ, 124, 1738
Rucinski, S. M., et al. 2005, AJ, 130, 767
Tokovinin, A. A., & Smekhov, M. G. 2002, A&A, 382, 118
Tokovinin, A., Thomas, S., Sterzik, M., & Udry, S. 2006, A&A, 450, 681
Vinkó, J., Hegedüs, T., & Hendry, P. D. 1996, MNRAS, 280, 489
Walker, R. L. 1973, Inf. Bull. Variable Stars, 855, 1
Zacharias, N., Urban, S. E., Zacharias, M. I., Wycoff, G. L., Hall, D. M., Monet, D. G., & Rafferty, T. J. 2004, AJ, 127, 3043